JACS
JOURNAL OF THE AMERICAN CHEMICAL SOCIETY

Communication

pubs.acs.org/JACS

Ionic Switch Induced by a Rectangular–Hexagonal Phase Transition in Benzenammonium Columnar Liquid Crystals

Bartolome Soberats,[†,‡] Masafumi Yoshio,[*,†] Takahiro Ichikawa,[§] Xiangbing Zeng,[⊥,¶] Hiroyuki Ohno,[§] Goran Ungar,[*,⊥,¶] and Takashi Kato[*,†,‡]

[†]Department of Chemistry and Biotechnology, School of Engineering, The University of Tokyo, 7-3-1 Hongo, Bunkyo-ku, Tokyo 113-8656, Japan

[‡]CREST, JST, 4-1-8, Honcho, Kawaguchi, Saitama 332-0012, Japan

[§]Department of Biotechnology, Faculty of Engineering, Tokyo University of Agriculture and Technology, Nakacho, Koganei, Tokyo 184-8588, Japan

[⊥]Department of Materials Science and Engineering, University of Sheffield, Sheffield S13JD, United Kingdom

[¶]Department of Physics, Zheijiang Sci-Tech University, Hangzhou 310018, China

Supporting Information

ABSTRACT: We demonstrate switching of ionic conductivities in wedge-shaped liquid-crystalline (LC) ammonium salts. A thermoreversible phase transition between the rectangular columnar (Col_r) and hexagonal columnar (Col_h) phases is used for the switch. The ionic conductivities in the Col_h phase are about four orders of magnitude higher than those in the Col_r phase. The switching behavior of conductivity can be ascribed to the structural change of assembled ionic channels. X-ray experiments reveal a highly ordered packing of the ions in the Col_r phase, which prevents the ion transport.

The use of self-assembly of liquid-crystalline (LC) molecules[1] possessing ionic,[2] electronic,[3] and photonic[4] functions is a promising approach to the development of soft functional materials with dynamic functions. The fluid LC assembled structures can be changed in response to external stimuli such as light irradiation,[5] the addition of chemicals,[6] application of mechanical pressure,[7] and application of an electric field.[8] The switch of functions using induced structural changes is an emerging research area.[5−9] Switching of electric current and photoluminescence has been studied for π-conjugated LC materials.[3,4,9] However, achieving switching of ionic conductivity is a challenging task because of the difficulty in the design of nanostructured materials forming ion-channels with stimuli responsiveness.[10] Percec and co-workers systematically studied a series of tapered crown ether−salt and oligo(ethylene oxide)−salt complexes exhibiting columnar LC phases.[2a−f] They first demonstrated a large amplitude change in the ionic conductivities from 10^{-12} to 10^{-8} S cm^{-1}, which was driven by the thermal phase transition from the crystal to LC columnar phase.[2a] Our intention here is to design columnar ionic liquid crystals exhibiting a large difference on the ionic conductivities accompanied by the change in the packing of the ionic species upon the thermal LC−LC phase transitions, which could lead to the development of new ion-based sensors and actuators.

Herein, we report on a thermal switch of ionic conductivities based on columnar LC assemblies of ammonium salts **1** and **2** (Figure 1). The change in ionic conductivities by four orders of magnitude is driven by the thermotropic rectangular columnar (Col_r)−hexagonal columnar (Col_h) LC phase transition (Figure 1b). The Col_r phases of compounds **1** and **2** exhibit remarkably lower conductivities than those in the Col_h phases (Figure 1b). Figure 2 demonstrates reversible switching of ionic conductivities for compound **1** during temperature cycling between 120 and 150 °C. The Col_r−Col_h and Col_h−Col_r phase transitions occur at 140 and 139 °C on heating and cooling, respectively. During the four successive heating−cooling cycles lasting 120 min, compound **1** exhibits a low conductivity state (ca. 10^{-8} S cm^{-1}) in the Col_r phase at 120 °C and a high

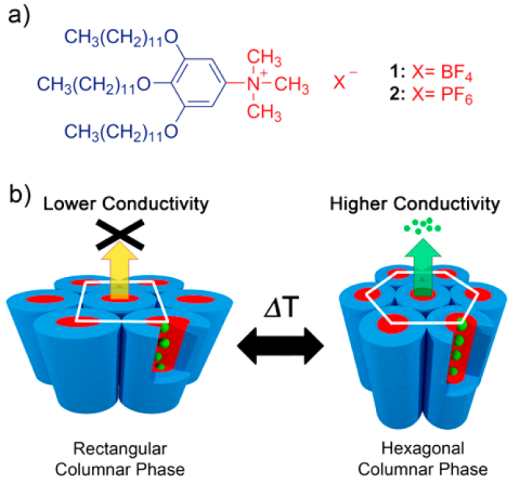

Figure 1. (a) Molecular structures of wedge-shaped ammonium salts **1** and **2**. (b) Schematic illustration of ionic switch based on structural change between hexagonal and rectangular columnar LC phases.

Received: April 23, 2015
Published: September 29, 2015

DOI: 10.1021/jacs.5b09076
J. Am. Chem. Soc. 2015, 137, 13212−13215

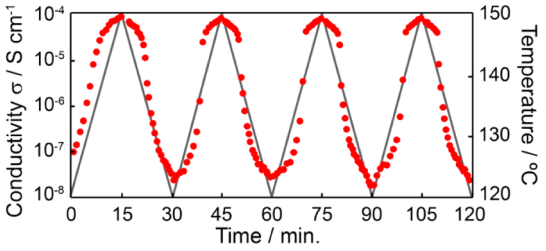

Figure 2. Ionic conductivity (red dots) of **1** and temperature (solid black line) as functions of time. Higher conductivities are recorded at 150 °C in the hexagonal columnar (Col_h) phase and lower conductivities at 120 °C in the rectangular columnar (Col_r) phase. The heating and cooling rates were 2 °C min^{-1}.

conductivity state (ca. 10^{-4} S cm^{-1}) in the Col_h phase at 150 °C.

We previously reported on the development of 3,4,5-trialkoxybenzyl-ammonium, -phosphonium, and -imidazolium LC ionic conductors forming columnar and bicontinuous cubic LC assemblies.[2j,k,11] On the basis of this research, we expected that the direct link between the fan-shaped phenyl ring and quaternary ammonium moiety would lead to a change in molecular packing and hence ionic conductivity.[12] Our current molecular design is a wedge-shaped trimethylbenzenammonium cation with BF_4 (**1**) and PF_6 (**2**) counteranions, respectively (Figure 1a and Supporting Information). The phase transition behavior of compounds **1** and **2** was determined by differential scanning calorimetry (DSC) and polarizing optical microscope observations (Supporting Information) together with X-ray diffraction (XRD) measurements (Supporting Information). We found that derivative **1** exhibits two rectangular columnar LC phases (Col_{r1} and Col_{r2}) at lower temperatures and a Col_h phase at higher temperatures (Table 1 and Supporting Information). On the other hand, compound **2** shows one Col_r (Col_{r2}) and a Col_h LC phases (Table 1 and Supporting Information). The DSC thermogram of **1** shows four transition peaks on heating, which correspond to the crystal–Col_{r1}, Col_{r1}–Col_{r2}, Col_{r2}–Col_h, and Col_h–isotropic phase transitions, respectively (Table 1 and Supporting Information). It should be noted that compound **1** exhibited higher stability than the benzylammonium derivatives.

The ionic conductivities of compounds **1** and **2** were examined as a function of temperature and compared to those of previously reported benzyltrimethylammonium salt **3** (Figure 3).[11a] It is significant that an abrupt conductivity jump, from 10^{-8} S cm^{-1} to 10^{-4} S cm^{-1}, is triggered by the Col_{r2}–Col_h transition for compounds **1** and **2** (Figure 3a). Between 120 and 144 °C, the ionic conductivity of **1** increases 1800 times, while between 114 and 128 °C, the conductivity of **2** increases 1200 times. In contrast, benzyltrimethylammonium derivative **3**, which exhibits only Col_h phase from 60 to 207 °C

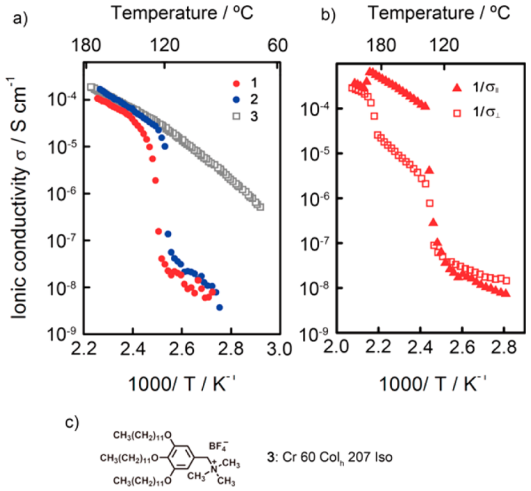

Figure 3. (a) Ionic conductivities as a function of temperature of compounds **1**–**3** in the columnar phases with polydomain orientations. (b) Ionic conductivities parallel ($\sigma_{\parallel}$) and perpendicular ($\sigma_{\perp}$) to the columnar axis of **1** with uniaxial orientation of the columns. The heating rate is 2 °C min^{-1}. (c) Molecular structure and LC behavior of compound **3**.

(Figure 3c), shows only a gradual increase in conductivity with increasing temperature (Figure 3a).[11a] For example, the value of conductivity for **3** changes from 2×10^{-5} to 7×10^{-5} S cm^{-1} when heated from 120 to 150 °C (Figure 3a and Supporting Information). The conductivities of **1** change from 10^{-8} to 10^{-4} S cm^{-1} in the same temperature range (Figures 2 and 3a). It is noteworthy that the ionic conductivities of compounds **1**–**3** in the Col_h phases have similar values (Figure 3a).

Anisotropic ionic conductivities were measured for the macroscopically aligned samples of **1** in the columnar phases on heating (Figure 3b and Supporting Information). The hexagonally ordered columns were oriented in two directions parallel and perpendicular to the comb-shaped gold electrodes by applying shear force. In the Col_h phase, the conductivities parallel to the columnar axis ($\sigma_{\parallel}$) are one order of magnitude higher than those of perpendicular to the columnar axis ($\sigma_{\perp}$). In contrast, no anisotropy of conductivities is observed in the Col_r phase; nevertheless, the two uniaxial columnar orientations achieved in the Col_h phase are maintained in the Col_r phase (Figure 3b). These results suggest that the anisotropic ion-transport pathways formed in the Col_h phase could be deformed and lost in the Col_r phase.

Previously, we reported on the ion conduction behavior of wedge-shape ionic liquid crystals in columnar and bicontinuous cubic phases.[2j,k,11] The formation of ion transport channels was observed in the bicontinuous cubic phases of benzyltriethylammonium based liquid crystals.[11a,13] Compounds **1** and **2** were examined by powder XRD and grazing incidence small-

Table 1. Thermal Properties of Compounds 1 and 2

compound	phase transition behavior[a]								
1	Cr	43 (20.6)	Col_{r1}	87 (0.2)	Col_{r2}	140 (8.1)	Col_h	196 (2.0)	Iso
2	Cr_1	53 (12.9)	Cr_2	89 (3.2)	Col_{r2}	122 (5.5)	Col_h	168 (1.4)	Iso

[a]Phase transition temperatures (°C) and enthalpies (kJ mol^{-1}, given in parentheses) determined by DSC (second heating, scan rate: 10 °C min^{-1}) and supported by polarizing optical microscope observation. Cr, crystal; Col_{r1}, Col_{r2}, columnar rectangular; Col_h, columnar hexagonal; Iso, isotropic.

DOI: 10.1021/jacs.5b09076
J. Am. Chem. Soc. 2015, 137, 13212–13215

and wide-angle X-ray scattering (GISAXS and GIWAXS) measurements (Figure 4 and Supporting Information). The

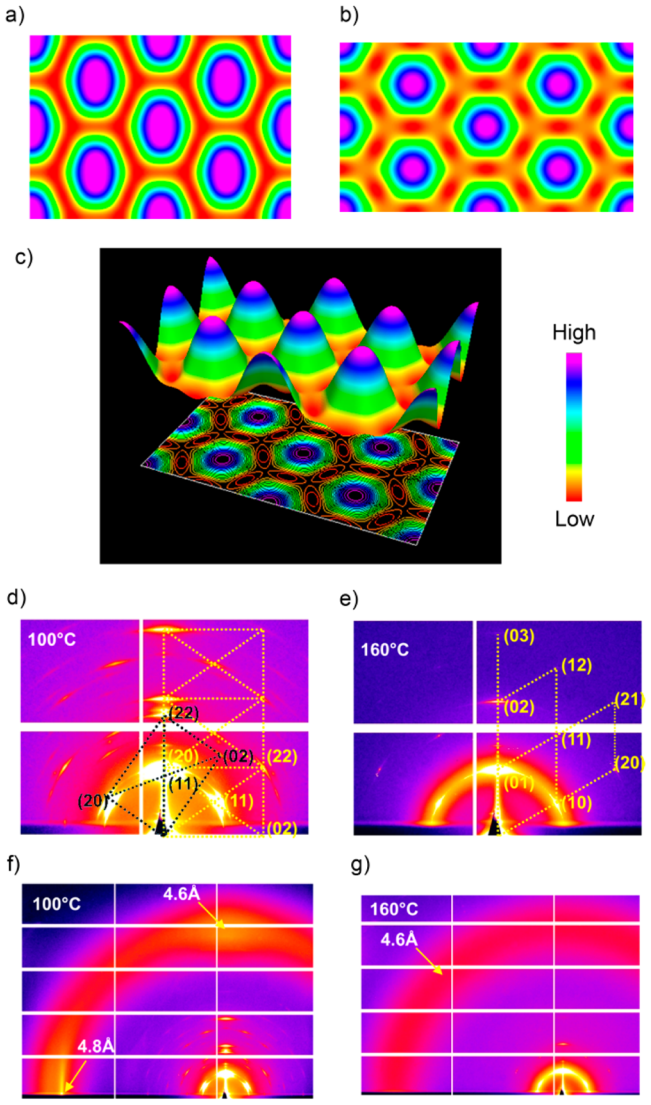

Figure 4. (a–c) EDMs $\rho(x,y)$ of compound **1** reconstructed from the powder XRD intensities (a) at 100 °C (Col_{r2} phase) and (b) at 160 °C (Col_h phase). (c) The 3D representation of the EDM of the Col_h phase of **1** at 160 °C. (d–g) GISAXS and GIWAXS patterns of a thin film of **1** on silicon: (d) GISAXS recorded at 100 °C (Col_{r2} phase) and (e) at 160 °C (Col_h phase). (f) GIWAXS recorded at 100 °C (Col_{r2} phase) and (g) at 160 °C (Col_h phase). The 2D reciprocal lattice is superimposed on the GISAXS patterns, but in the Col_r phases, only the nodes corresponding to reflections allowed by the *c2mm* plane group are shown.

XRD pattern of compound **1** at 160 °C shows one strong and two weak peaks corresponding to the (10), (11), and (20) reflections of the Col_h phase (Supporting Information). In contrast, the XRD pattern of compound **1** at 100 °C shows two intense and eight weak peaks in the small-angle region (Supporting Information) corresponding to a Col_r phase. Electron density maps (EDMs) $\rho(x,y)$ were reconstructed from the powder XRD intensities for compounds **1** and **2** in their Col_r and Col_h phases (Figure 4a–c and Supporting Information). Figure 4, panels a and b display the 2D representation of the reconstructed EDMs of compound **1** at 100 (Col_{r2}) and 160 °C (Col_h), respectively. The 3D representations of the EDMs are shown in Figure 4, panel c and the Supporting Information. The EDMs in the Col_r and Col_h phases show that the higher electron densities are concentrated in the center of the columns, while lower density areas occupy the columnar periphery. This observation suggests that the aromatic cores and anions of **1** and **2** are localized in the center of the columns, which is consistent with previous reports on LC nanosegregated ion transport materials.[11a] The map of the Col_{r2} phase of **1** shows an oval shape of the electron-rich area of the columns, while the shape becomes circular in the Col_h phase (Figure 4a–c). The number of molecules per columnar cross-section (4.9 Å) was estimated to be around four for both Col_{r2} and Col_h phases (Supporting Information). These results indicate that the arrangement of the molecules inside the columns significantly changes by the Col_r–Col_h phase transition.

All grazing incidence patterns show planar alignment of the columns on silicon substrate (Figure 4d–g and Supporting Information). The GIWAXS and GISAXS patterns of **1** at 160 °C (Figure 4e,g) confirm the Col_h structure with the lattice parameter a = 3.4 nm (Supporting Information), while the Col_{r2} phase at 100 °C has the centered rectangular *c2mm* symmetry (all reflections with $h + k$ = odd are missing) (Figure 4d,f and Supporting Information). Significantly, in the Col_{r2} phase of compounds **1** and **2**, the GIWAXS patterns show a strong vertical streak on the horizon corresponding to a regular intracolumnar periodicity of 0.48 and 0.50 nm for compounds **1** and **2**, respectively (Figure 4f and Supporting Information). Had the columns been aligned homeotropically, that is, normal to the film plane, all intensity distributed around the equatorial circle in reciprocal space would have been condensed near the pole, that is, on the meridian, and the streak would have appeared much stronger. Such intensity can only be due to regular stacking of the electron-rich counteranions along the column axis. We assume that cations and anions occupy a fixed position inside the rectangular columnar structure, and therefore they are not mobile. Such regular stacking of the ions is consistent with a low mobility and hence low conductivity. In contrast, only diffuse liquid-like scattering is observed in the GIWAXS patterns in the Col_h phase of **1** (Figure 4g). These results are consistent with those on our previous Col_h LC materials.[11a] A detailed characterization of the organized structure of ions in the Col_r phase is currently under way and will be reported in the future.

In summary, the new design of ammonium-based ionic liquid crystals led to an unprecedented conductivity switch between the low-conductivity "OFF" state in the Col_r phase and a high-conductivity "ON" state in the Col_h phase. This switching relies on the transition between the Col_r phase, preventing ion transport, and the conductive Col_h phase. The additional advantage of this system as a potential thermal switch is the high reversibility of the Col_r–Col_h phase transition and the preservation of the orientation of the columns. We expect that switchable ion-conductive materials could be used in molecular-based ionic devices.

■ ASSOCIATED CONTENT

Supporting Information

The Supporting Information is available free of charge on the ACS Publications website at DOI: 10.1021/jacs.5b09076.

DOI: 10.1021/jacs.5b09076
J. Am. Chem. Soc. 2015, 137, 13212–13215

Detailed experimental procedures and materials characterization (PDF)

AUTHOR INFORMATION

Corresponding Authors

*kato@chiral.t.u-tokyo.ac.jp
*yoshio@chembio.t.u-tokyo.ac.jp
*g.ungar@sheffield.ac.uk

Notes

The authors declare no competing financial interest.

ACKNOWLEDGMENTS

This study was partially supported by the Funding Program for World-Leading Innovative R&D on Science and Technology (FIRST) from the Cabinet Office, Government of Japan. This work was also partially supported by a Grant-in-Aid for Scientific Research (No. 22107003) in the Innovative Area of "Fusion Materials" (Area No. 2206) and Grant-in-Aid for The Global COE Program "Chemistry Innovation through Cooperation of Science and Engineering" from The Ministry of Education, Culture, Sports, Science, and Technology (MEXT). Support is also acknowledged from the "1000 Talents" program of the Government of China and the Joint NSF-EPSRC PIRE project "RENEW" (EPSRC Grant No. EP_K034308). We thank Dr. G. Nisbet and Prof. S. Collins of I16 at Diamond Light Source for help with setting up the synchrotron experiments.

REFERENCES

(1) (a) Goodby, J. W.; Collings, P. J.; Kato, T.; Tschierske, C.; Gleeson, H.; Raynes, P. *Handbook of Liquid Crystals*, 2nd ed.; Wiley-VCH: Weinheim, 2014. (b) Kato, T.; Mizoshita, N.; Kishimoto, K. *Angew. Chem., Int. Ed.* **2006**, *45*, 38−68. (c) Tschierske, C. *J. Mater. Chem.* **1998**, *8*, 1485−1508. (d) Tschierske, C. *Chem. Soc. Rev.* **2007**, *36*, 1930−1970. (e) Kato, T. *Science* **2002**, *295*, 2414−2418. (f) Ungar, G.; Liu, Y.; Zeng, X.; Percec, V.; Cho, W. D. *Science* **2003**, *299*, 1208−1211. (g) Deschenaux, R.; Donnio, B.; Guillon, D. *New J. Chem.* **2007**, *31*, 1064−1073. (h) Gin, D. L.; Pecinovsky, C. S.; Bara, J. E.; Kerr, R. L. *Struct. Bonding (Berlin)* **2008**, *128*, 181−222. (i) Rosen, B. M.; Wilson, C. J.; Wilson, D. A.; Peterca, M.; Imam, M. R.; Percec, V. *Chem. Rev.* **2009**, *109*, 6275−6540.

(2) (a) Percec, V.; Johansson, G.; Heck, J.; Ungar, G.; Batty, S. *J. Chem. Soc., Perkin Trans. 1* **1993**, 1411−1420. (b) Ungar, G.; Batty, S. V.; Percec, V.; Heck, J.; Johansson, G. *Adv. Mater. Opt. Electron.* **1994**, *4*, 303−313. (c) Tomazos, D.; Out, G.; Heck, J. A.; Johansson, G.; Perce, V.; Möller, M. *Liq. Cryst.* **1994**, *16*, 509−527. (d) Percec, V.; Heck, J. A.; Tomazos, D.; Ungar, G. *J. Chem. Soc., Perkin Trans. 2* **1993**, 2381−2388. (e) Percec, V.; Heck, J.; Tomazos, D.; Falkenberg, F.; Blackwell, H.; Ungar, G. *J. Chem. Soc., Perkin Trans. 1* **1993**, 2799−2811. (f) Percec, V.; Johansson, G.; Ungar, G.; Zhou, J. *J. Am. Chem. Soc.* **1996**, *118*, 9855−9866. (g) Kato, T. *Angew. Chem.* **2010**, *122*, 8019−8021. (h) Kerr, R. L.; Miller, S. A.; Shoemaker, R. K.; Elliott, B. J.; Gin, D. L. *J. Am. Chem. Soc.* **2009**, *131*, 15972−15973. (i) Yoshio, M.; Mukai, T.; Kanie, K.; Yoshizawa, M.; Ohno, H.; Kato, T. *Adv. Mater.* **2002**, *14*, 351−354. (j) Ichikawa, T.; Yoshio, M.; Hamasaki, A.; Mukai, T.; Ohno, H.; Kato, T. *J. Am. Chem. Soc.* **2007**, *129*, 10662−10663. (k) Yoshio, M.; Kagata, T.; Hoshino, K.; Mukai, T.; Ohno, H.; Kato, T. *J. Am. Chem. Soc.* **2006**, *128*, 5570−5577. (l) Binnemans, K. *Chem. Rev.* **2005**, *105*, 4148−4204. (m) Cho, B.-K.; Jain, A.; Gruner, S. M.; Wiesner, U. *Science* **2004**, *305*, 1598−1601. (n) Imam, M. R.; Peterca, M.; Edlund, U.; Balagurusamy, V. S. K.; Percec, V. *J. Polym. Sci., Part A: Polym. Chem.* **2009**, *47*, 4165−4193. (o) Högberg, D.; Soberats, B.; Uchida, S.; Yoshio, M.; Kloo, L.; Segawa, H.; Kato, T. *Chem. Mater.* **2014**, *26*, 6496−6502. (p) Sakuda, J.; Hosono, E.; Yoshio, M.; Ichikawa, T.; Matsumoto, T.; Ohno, H.; Zhou, H. S.; Kato, T. *Adv. Funct. Mater.* **2015**, *25*, 1206−1212. (q) Yamanaka, N.; Kawano, R.; Kubo, W.; Kitamura, T.; Wada, Y.; Watanabe, M.; Yanagida, S. *Chem. Commun.* **2005**, 740−742.

(3) (a) Tsao, H. N.; Räder, H. J.; Pisula, W.; Rouhanipour, A.; Müllen, K. *Phys. Status Solidi A* **2008**, *205*, 421−429. (b) Sergeyev, S.; Pisula, W.; Geerts, Y. H. *Chem. Soc. Rev.* **2007**, *36*, 1902−1929. (c) Bushby, R. J.; Lozman, O. R. *Curr. Opin. Solid State Mater. Sci.* **2002**, *6*, 569−578. (d) Boden, N.; Bushby, R. J.; Clements, J. *J. Chem. Phys.* **1993**, *98*, 5920−5931. (e) Percec, V.; Glodde, M.; Bera, T. K.; Miura, Y.; Shiyanovskaya, I.; Singer, K. D.; Balagurusamy, V. S. K.; Heiney, P. A.; Schnell, I.; Rapp, A.; Spiess, H.-W.; Hudson, S. D.; Duan, H. *Nature* **2002**, *419*, 384−387. (f) Yazaki, S.; Funahashi, M.; Kagimoto, J.; Ohno, H.; Kato, T. *J. Am. Chem. Soc.* **2010**, *132*, 7702−7708. (g) Yasuda, T.; Shimizu, T.; Liu, F.; Ungar, G.; Kato, T. *J. Am. Chem. Soc.* **2011**, *133*, 13437−13444. (h) Kumar, S. *Isr. J. Chem.* **2012**, *52*, 820−829. (i) Pisula, W.; Zorn, M.; Chang, J. Y.; Müllen, K.; Zentel, R. *Macromol. Rapid Commun.* **2009**, *30*, 1179−1202. (j) Hoeben, F. J. M.; Jonkheijm, P.; Meijer, E. W.; Schenning, A. P. H. J. *Chem. Rev.* **2005**, *105*, 1491−1546. (k) Bisoyi, H. K.; Kumar, S. *Chem. Soc. Rev.* **2011**, *40*, 306−319.

(4) (a) Sagara, Y.; Kato, T. *Nat. Chem.* **2009**, *1*, 605−610. (b) Hong, Y.; Lam, J. W. Y.; Tang, B. Z. *Chem. Soc. Rev.* **2011**, *40*, 5361−5388.

(5) (a) Ikeda, T. *J. Mater. Chem.* **2003**, *13*, 2037−2057. (b) Kawatsuki, N. *Chem. Lett.* **2011**, *40*, 548−554. (c) Soberats, B.; Uchida, E.; Yoshio, M.; Kagimoto, J.; Ohno, H.; Kato, T. *J. Am. Chem. Soc.* **2014**, *136*, 9552−9555. (d) Kosa, T.; Sukhomlinova, L.; Su, L.; Taheri, B.; White, T. J.; Bunning, T. J. *Nature* **2012**, *485*, 347−349. (e) Zakrevskyy, Y.; Stumpe, J.; Faul, C. F. J. *Adv. Mater.* **2006**, *18*, 2133−2136.

(6) (a) Soberats, B.; Yoshio, M.; Ichikawa, T.; Taguchi, S.; Ohno, H.; Kato, T. *J. Am. Chem. Soc.* **2013**, *135*, 15286−15289. (b) Tan, B. H.; Yoshio, M.; Kato, T. *Chem. - Asian J.* **2008**, *3*, 534−541. (c) Su, X.; Voskian, S.; Hughes, R. P.; Aprahamian, I. *Angew. Chem., Int. Ed.* **2013**, *52*, 10734−10739. (d) Lowe, A. M.; Abbott, N. L. *Chem. Mater.* **2012**, *24*, 746−758.

(7) Sagara, Y.; Kato, T. *Angew. Chem., Int. Ed.* **2011**, *50*, 9128−9132.

(8) Beneduci, A.; Cospito, S.; La Deda, M.; Veltri, L.; Chidichimo, G. *Nat. Commun.* **2014**, *5*, 1−8.

(9) Funahashi, M.; Zhang, F. P.; Tamaoki, N. *Adv. Mater.* **2007**, *19*, 353−358.

(10) (a) Peterca, M.; Percec, V.; Dulcey, A. E.; Nummelin, S.; Korey, S.; Ilies, M.; Heiney, P. A. *J. Am. Chem. Soc.* **2006**, *128*, 6713−6720. (b) Pecinovsky, C. S.; Hatakeyama, E. S.; Gin, D. L. *Adv. Mater.* **2008**, *20*, 174−178.

(11) (a) Ichikawa, T.; Yoshio, M.; Hamasaki, A.; Taguchi, S.; Liu, F.; Zeng, X. B.; Ungar, G.; Ohno, H.; Kato, T. *J. Am. Chem. Soc.* **2012**, *134*, 2634−2643. (b) Yoshio, M.; Ichikawa, T.; Shimura, H.; Kagata, T.; Hamasaki, A.; Mukai, T.; Ohno, H.; Kato, T. *Bull. Chem. Soc. Jpn.* **2007**, *80*, 1836−1841.

(12) Kouwer, P. H. J.; Swager, T. M. *J. Am. Chem. Soc.* **2007**, *129*, 14042−14052.

(13) Frise, A. E.; Ichikawa, T.; Yoshio, M.; Ohno, H.; Dvinskikh, S. V.; Furo, I.; Kato, T. *Chem. Commun.* **2010**, *46*, 728−730.

DOI: 10.1021/jacs.5b09076
J. Am. Chem. Soc. 2015, 137, 13212−13215